The scattering is dominated by the average structure of the adsorbed layer; there is no observable contribution from fluctuations as has been recently suggested. The structure of the adsorbed layer does not follow any simple scaling law. Using SANS data away from the zero contrast condition is problematical and in general unsatisfactory due to difficulties of obtaining data for the Guinier approximation and because of scattering from the substrate itself. The experimental strategy suggested by Auvray and de Gennes is therefore impractical, and the best experimental results have been obtained at zero contrast.

Acknowledgment. We wish to thank the SERC (T. G.H. and K.R.) and the United Kingdom Department of Energy (K.R.) for financial assistance and the ILL, Grenoble, for the use of SANS facilities with particular thanks to Albert Wright for his help in collecting the SANS data. We are also grateful to Brian Vincent for his continued interest in this work.

Registry No. PEO, 25322-68-3; dPS, 27732-42-9; neutron, 12586-31-1.

References and Notes

(1) Ottewill, R. H. In *Colloidal Dispersions*; Goodwin, J. W., Ed.; Royal Society of Chemistry: London, 1982; p 143.
(2) Cebula, D. J.; Ottewill, R. H.; Ralston, J.; Pusey, P. N. *J. Chem. Soc., Faraday Trans. 1* **1981**, *77*, 2585.
(3) Cosgrove, T.; Cohen Stuart, M. A.; Vincent, B. *Adv. Colloid Interface Sci.* **1986**, *24*, 143.
(4) Crowley, T. L. D.Phil. Thesis, University of Oxford, 1984.
(5) Auvray, L.; de Gennes, P. G. *Europhys. Lett.* **1986**, *2*, 647.
(6) Barnett, K. G.; Cosgrove, T.; Crowley, T. L.; Tadros, Th. F.; Vincent, B. In *The Effects of Polymers on Dispersion Stability*; Tadros, Th. F., Ed.; Academic: London, 1981; p 183.
(7) Barnett, K. G.; Cosgrove, T.; Vincent, B.; Burgess, A. N.; Crowley, T. L.; King, T.; Turner, J. D.; Tadros, Th. F. *Polymer* **1981**, *22*, 283.
(8) Cosgrove, T.; Crowley, T. L.; Vincent, B. In *Adsorption from Solution*; Ottewill, R. H., Rochester, C. H., Smith, A. L., Eds.; Academic: London, 1983; p 287.
(9) Boomgard, Th. van den; King, T. A.; Tadros, Th. F.; Tang, H.; Vincent, B. *J. Colloid Interface Sci.* **1978**, *66*, 68.
(10) Porod, G. *Kolloid Z.* **1951**, *124*, 83.
(11) Thomas, R. K.; Willat, A. J.; Crowley, T. L., to be submitted for publication in *Mol. Phys.*
(12) Auvray, L.; Cotton, J. P. *Macromolecules* **1987**, *20*, 202.
(13) Schaefer, D. W. *Polymer* **1984**, *25*, 387.

Potentiometric Titration of Xanthan

Lina Zhang,† Toshiyuki Takematsu, and Takashi Norisuye*

Department of Macromolecular Science, Osaka University, Toyonaka, Osaka 560, Japan.
Received February 23, 1987

ABSTRACT: Potentiometric titration data were obtained for two samples of rigid double-helical xanthan in aqueous sodium chloride at salt concentrations C_s of 0.01, 0.02, 0.05, and 0.1 M at 25 °C, and from their comparison with typical theories along with some theoretical considerations the following conclusions were derived. (1) The solution of the complete Poisson–Boltzmann equation for a uniformly charged cylinder fails to describe the titration data, unless an unreasonably large value is chosen for the radius of the xanthan double helix. (2) The well-known expression $\mathrm{pH} - \log [\alpha/(1-\alpha)] - \mathrm{p}K_0 = -2\alpha\sum_j \log u_j$ for a long rod with randomly distributed discrete charges agrees with the result from the linear Ising model at degrees of ionization α of $^1/_2$ and 1, where $\mathrm{p}K_0$ is the logarithmic intrinsic dissociation constant and u_j, the statistical weight for the electrostatic interaction of a given ionized group with its jth neighbor group. (3) This equation combined with the Debye–Hückel screened Coulomb potential, an approximation to the pair interaction potential, describes the xanthan data only at the two higher C_s of 0.05 and 0.1 M. Its failure at the lower C_s is attributable to this approximation. Similar analysis of the published data for α-helical poly(glutamic acid), another rodlike polyelectrolyte, led to essentially conclusions 1 and 3.

Introduction

The pH of a polyelectrolyte solution is usually expressed by [1-3]

$$\Delta \mathrm{p}K \equiv \mathrm{pH} - \log (\alpha/1-\alpha) - \mathrm{p}K_0 = 0.434 e\psi/kT \qquad (1)$$

where α is the degree of ionization of ionizable groups in the polymer, K_0 the intrinsic dissociation constant of a group ($\mathrm{p}K_0 = -\log K_0$), e the protonic charge, ψ the electrostatic potential at a point of a charge on the polymer surface, k the Boltzmann constant, and T the absolute temperature. For uniformly charged long cylinders, numerical values[4-7] of ψ were obtained from the complete Poisson–Boltzmann equation, while for discretely charged rods, various approximate expressions[8-15] for ψ (or more generally $\Delta \mathrm{p}K$) were derived on different assumptions. These theories of ψ or $\Delta \mathrm{p}K$ may be checked if data of $\mathrm{pH} - \log (\alpha/1-\alpha)$ are obtained for polyelectrolytes having an intrinsically rigid backbone, i.e., those rigid even at high salt concentrations.

† Present Address: Department of Chemistry, Wuhan University, Wuchang, the People's Republic of China.

The present paper reports such an experimental study made on xanthan, a bacterial polysaccharide with ionic side chains, in aqueous sodium chloride (NaCl) of salt concentrations C_s of 0.01, 0.02, 0.05, and 0.1 M. This polysaccharide, whose repeating units are shown in Figure 1, should be eligible for use as the test sample, since its sodium salt has recently been shown to dissolve in aqueous NaCl as a rigid double helix[16-21] with a large persistence length of about 100 nm at infinite ionic strength.[22] We note that although comparisons between theory and experiment were already made by many workers,[3-6,12-15,23-25] the conclusions drawn were not always definite since intrinsically flexible polyelectrolytes were used except α-helical poly(glutamic acid).

Experimental Section

Potentiometric Titration. The previously investigated xanthan samples,[26] X12-2-3 and X14-2-3 with weight-average molecular weights of 3.31×10^5 and 7.44×10^5, respectively (both in the dimerized acid form), were used. Either sample was dissolved in deionized water at about 5 °C, and the solution was passed through a mixed-bed ion exchanger (Amberlite IR-120 + IRA-410), with the temperature of the solution kept at about 5

0024-9297/87/2220-2882$01.50/0

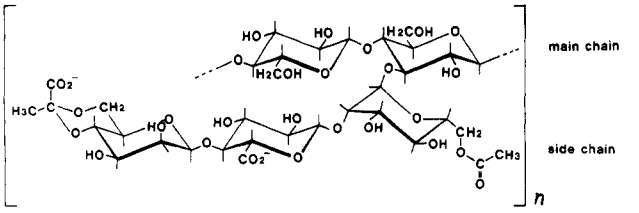

Figure 1. Repeating unit of xanthan. About one-third of the terminal residues of the side chains is pyruvated in the samples used in the previous[17-19,22] and present work.

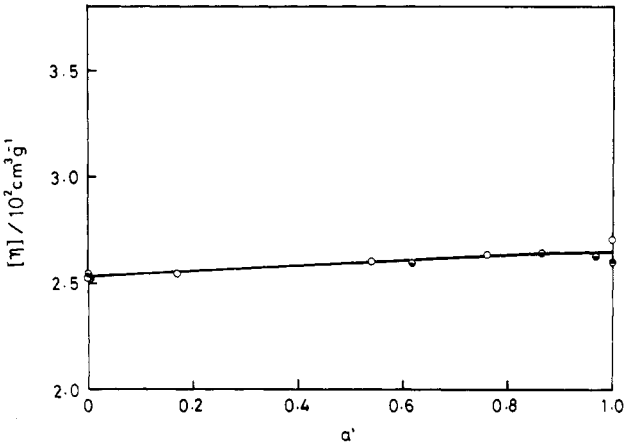

Figure 2. Dependence of intrinsic viscosity on degree of neutralization for xanthan sample X12-2-3 in aqueous NaCl of C_s = 0.01 (○), 0.05 (◒), and 0.1 M (◒) at 25 °C.

°C. To the solution of acid form xanthan so prepared, aqueous NaCl was added to obtain a test solution of a desired C_s. The sodium chloride used was recrystalized twice by the standard method.

Each test solution (10 cm³) was titrated at 25 °C under a nitrogen atmosphere with 0.100 N sodium hydroxide (NaOH) containing NaCl of the same C_s as that in the xanthan solution. The titrant was delivered by using a Gilmont digital microburet (Type S4100A) with a capacity of 0.25 cm³ and a vernier division of 0.000 01 cm³. The concentration c_p of carboxylic acid groups was determined from that of NaOH in the solution at the end point of the titration; the amount of the titrant required for complete neutralization was at most 0.4 cm³. For pH measurements, use was made of a Beckman ϕ 70 pH meter calibrated with standard buffer solutions of pH 4.01 and 6.86.

The concentration $[H^+]$ of free hydrogen ions at a given C_s and pH was evaluated from the calibration curve of $[H^+]$ vs. pH determined by titrating similarly aqueous hydrochloric acid (HCl) (10 cm³) containing NaCl of the same C_s.[27] From the $[H^+]$ so estimated and the degree of neutralization α', α was calculated according to the relation

$$\alpha = \alpha' + ([H^+] - [OH^-])/c_p \quad (2)$$

with the small contribution from $[OH^-]$ (the concentration of free hydroxyl ions) neglected; α', $[H^+]$, and c_p were all corrected for changes (≲4%) in the volumes of the xanthan and HCl solutions accompanying addition of the titrant.

Viscometry. In our previous work,[26] it was found that the intrinsic viscosities $[\eta]$ of Na salt samples X12-2-3 and X14-2-3 in aqueous NaCl of C_s = 0.01–0.5 M decreased by about 20% when solvent pH was lowered from about 6 to 2 by addition of HCl. Analysis of $[\eta]$ and radius of gyration data showed these decreases in $[\eta]$ to be due not to breaking of the double-helical structure of xanthan but to a decrease in the rigidity (expressed in terms of the persistence length) of the helix accompanying the uptake of hydrogen ions by xanthan. Thus, viscometry may be used for checking whether the rigidity of the double helix changes with α in the range of the present titration experiment.

We deemed such a check indispensable for our purpose mentioned in the Introduction, and determined $[\eta]$ of sample X12-2-3 in aqueous NaCl with different C_s's at 25 °C over the entire range of α'. The polymer mass concentration was calculated from c_p

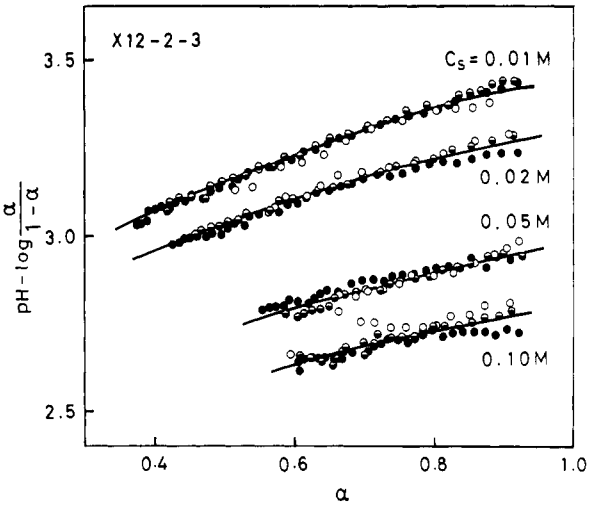

Figure 3. Titration data for xanthan sample X12-2-3 in aqueous NaCl of indicated C_s at 25 °C: (●) c_p = 0.0039 M; (◒) 0.0026 M; (○) 0.0013 M.

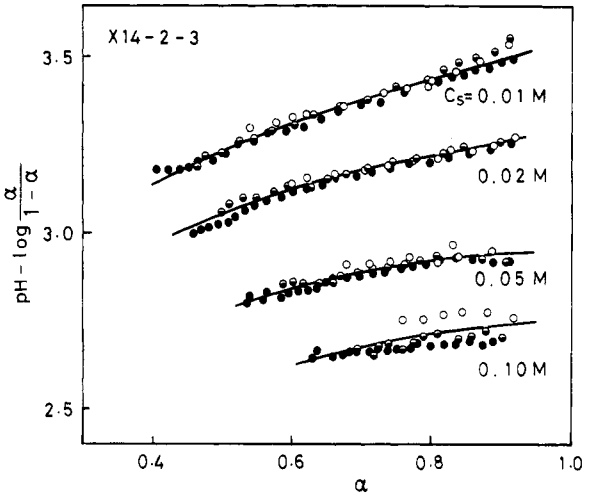

Figure 4. Titration data for xanthan sample X14-2-3 in aqueous NaCl of indicated C_s at 25 °C: (●) c_p = 0.0024 M; (◒) 0.0016 M; (○) 0.0008 M.

and the experimentally determined DS_{pyr} (the degree of pyruvation) of 0.34.[28]

Results

Figure 2 illustrates the dependence of $[\eta]$ on α' for sample X12-2-3 in aqueous NaCl of C_s = 0.01, 0.05, and 0.1 M. It can be seen that $[\eta]$ is essentially independent of C_s and almost constant throughout the entire range of α'. Thus, we may conclude that at least in the range of C_s studied, the xanthan double helix maintains its high rigidity[17-22] at α' = 1 down to α' = 0, i.e., the lowest α in the present titration study.

Figures 3 and 4 show pH – log $[\alpha/(1-\alpha)]$ plotted against α for samples X12-2-3 and X14-2-3 at different c_p and C_s. The data for either sample at fixed C_s are virtually independent of c_p and hence may be regarded as those at infinite dilution.

When the curves fitting these data were extended smoothly to α = 0, smaller pK_0 values were obtained at higher C_s. Such C_s dependence of pK_0 is consistent with the findings of Olander and Holtzer[29] and Mandel,[30] who showed pK_0 of poly(DL-glutamic acid) and poly(acrylic acid) to be a decreasing function of ionic strength.

Comparison between Theory and Experiment

Uniformly Charged Cylinder Model. Stigter[7] expressed his numerical solutions of the complete Poisson–

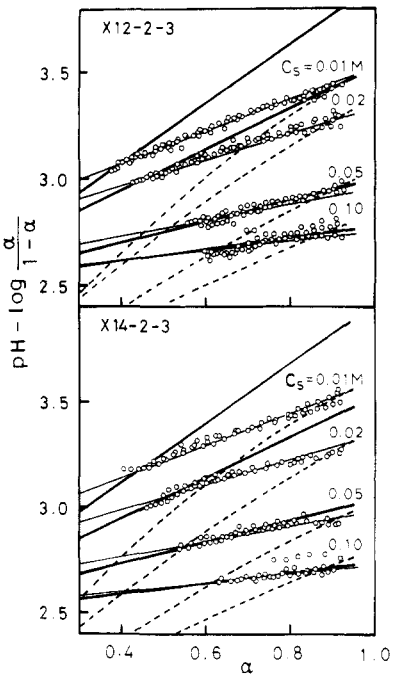

Figure 5. Comparison of titration data for xanthan with theoretical values: Dashed lines, eq 3 with a = 1.2 nm and σ = 2.85 nm^{-1}; thick solid lines, eq 6 (to $j = \infty$) with eq 8; thin solid lines, eq 6 (to j = 4) with eq 8.

Boltzmann equation for a long cylinder with uniform surface charge (referred to as the uniformly charged cylinder model) as

$$\psi_a = 2\sigma\alpha e K_0(\kappa a)/D\beta\kappa a K_1(\kappa a) \quad (3)$$

by introducing a factor β ($\geq$1) into the expression[31] derived from the linearized Poisson–Boltzmann equation. Here, ψ_a is the electrostatic potential at the distance a from the cylinder axis that small ions can approach the cylinder most closely (i.e., a = the radius of small ions + the radius b of the cylinder), σ is the linear charge density of the cylinder in the fully ionized state, $K_0(\kappa a)$ and $K_1(\kappa a)$ are the zeroth- and first-order modified Bessel functions of the second kind [$K_0(\kappa a)$ should not be confused with the intrinsic dissociation constant K_0], D is the dielectric constant of the solvent water, and κ is the reciprocal of the Debye length defined for univalent electrolytes by

$$\kappa^2 = 8\pi e^2 N_A C_s/1000DkT \quad (4)$$

with N_A being the Avogadro constant (C_s is expressed in units of mol L^{-1}). Values of β are tabulated as a function of $e\psi_a/kT$ and κa in Stigter's paper. The desired potential ψ (see eq 1) at the cylinder surface is related to ψ_a by[23,24,31]

$$\psi = \psi_a + 2\sigma\alpha e D^{-1} \ln (a/b) \quad (5)$$

but in the analysis below, it is assumed that $a = b$, as was done by previous investigators.[3,6,15,23-25]

The dashed lines in Figure 5 represent the theoretical values of $pK_0 + 0.434e\psi/kT$ [=pH − log (α/1 − α)] calculated from eq 3 for a ($=b$) = 1.2 nm[19] and σ = 2.85 nm^{-1} with pK_0 chosen properly (1.83–1.99) for either sample at each C_s; the σ value for the helical xanthan dimer was calculated from the relation $\sigma = 2(1 + DS_{pyr})/2h$ using DS_{pyr} = 0.34 and h (the axial translation per main-chain residue) = 0.47 nm.[17,19,26,32] We see that each dashed line rises very steeply with increasing α and cannot fit the data points at the corresponding C_s whatever value may be chosen for pK_0. Note that inclusion of the second term on the right-hand side of eq 5 leads to larger discrepancies. Close fits were found, when b was taken to be 4 nm. However, this value is more than 3 times the radius (1.2 ± 0.2 nm) of the xanthan double helix in dilute solution[18-20,26] or in the crystalline state.[32] Thus, it may be concluded that the Poisson–Boltzmann solution for a uniformly charged cylinder fails to describe the titration data for rigid double-helical xanthan, unless an unreasonably large value is chosen for the helix radius.

The observed discrepancies between the data and the dashed lines are too large to be accounted for by the presence of a hydration layer[33] (near the polyelectrolyte) or by approximations involved in the Poisson–Boltzmann equation.[34] It seems reasonable to attribute them to the approximation of smearing the actual discrete charges over the surface of the xanthan double helix.

Discrete Charge Model. A. Theoretical Considerations. Among many approximate titration equations[8-15] derived for an infinitely long rigid polyacid with discrete point charges, the one with the seemingly widest applicability is[15]

$$\Delta pK = -2\alpha \sum_{j=1}^{\infty} \log u_j \quad (6)$$

with

$$u_j = \exp(-w_{0,j}/kT) \quad (7)$$

Here, $w_{0,j}$ is the electrostatic interaction energy for a pair of a given ionizable group or site (the subscript 0) and its jth neighbor site (the subscript j), both in the ionized state, and is usually assumed to be represented by the Debye–Hückel (DH) screened Coulomb potential, i.e.,

$$w_{0,j} = (e^2/Dr_{0j}) \exp(-\kappa r_{0j}) \quad (8)$$

with r_{0j} being the distance between sites 0 and j. Equation 6 is based on the assumption that at any α the charges in the polymer are randomly distributed.

A titration equation free from this assumption should, in principle, be derived by the linear Ising method, but since the method requires an intractably high order matrix to be evaluated, its actual application has so far been limited to cases of a few or at most four nearest-neighbor interactions.[8-11,13,15,35] Minakata et al.[13,36] took another approach, in which they evaluated a few nearest-neighbor interactions rigorously by the Ising method and the other higher order interactions separately by an approximate method. Although such a separate calculation is not always well founded statistical mechanically, the idea of these authors is inviting since the effect of nonrandom distribution, which should be of short range, is taken into account, along with long-range electrostatic interactions.

On the basis of a similar idea and by use of some properties[11] of the grand partition function in the Ising method, we obtained an approximate expression

$$\Delta pK = \log [[(1 - \alpha)/\alpha] \times [1 + xu_1^{-1} \pm [(1 + xu_1^{-1})^2 - 1]^{1/2}]u_1^{-1}] - 2\alpha \sum_{j=2}^{\infty} \log u_j \quad (9)$$

which gives the same ΔpK values as those derived by the Ising method at particular α of $^1/_2$ and 1 (see the Appendix). In eq 9, x is defined by

$$x = \frac{1}{2}\left(\frac{\alpha}{1-\alpha} + \frac{1-\alpha}{\alpha} - 2\right) \quad (10)$$

and the sign ± is taken to be + for $\alpha > 0.5$ and − for $\alpha < 0.5$.

It can be shown that at α = 0, $^1/_2$, and 1 eq 6 and 9 are identical and that at other α their differences are no more than 0.02 in ΔpK unit for $u_1 > 0.5$ (i.e., $r_{01} > 0.8$ nm at a C_s of 0.01 M and 25 °C if expressed by using the DH

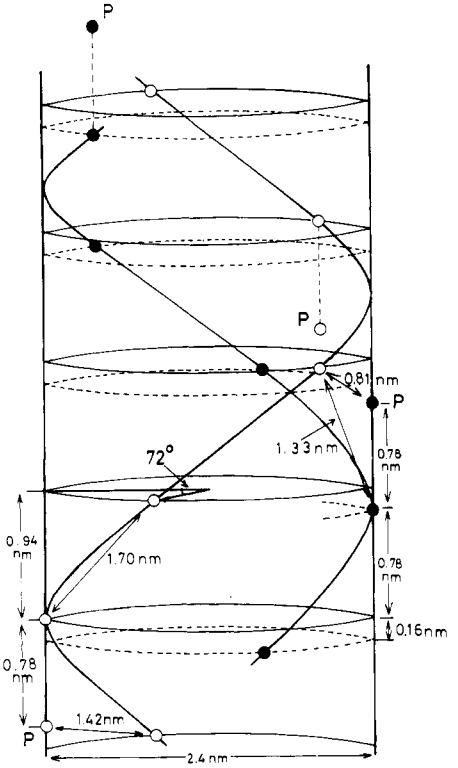

Figure 6. Locations of carboxylic acid groups on the surface of double-helical xanthan, estimated from the 5_1 antiparallel double-helix model of Okuyama et al.[32] P, pyruvic acid group.

potential with the bulk dielectric constant D). This indicates that if the closest distance between charges in the polyacid considered is greater than 0.8 nm and if $C_s \geq 0.01$ M, the assumption of random charge distribution introduces no significant error. In other words, under these conditions, eq 6 is essentially equivalent to a more rigorous eq 9, and both should be a very good approximation to the complete but yet-unknown Ising result. For the double helix of xanthan, the closest charge distance is 0.78 nm (see Figure 6), which is comparable to 0.8 nm. We therefore decided to compare eq 6 with our xanthan data ($C_s \geq 0.01$ M), regarding it as a typical theory for discretely charged rigid polyacids.

B. Analysis. Figure 6 schematically shows the locations of carboxylic acid groups in double-helical xanthan, estimated approximately from the 5_1 antiparallel double helix model.[32] We have assumed that the central one of every three side chains in each strand of the dimer has a pyruvic acid group (denoted by P in the figure), i.e., a DS_{pyr} of $^1/_3$, close to the experimental value of 0.34. This assumption completely specifies the locations[37] of all the carboxylic acid groups within either strand, but there are three different ways of assembling the two strands; note that one of them is shown in Figure 6. Taking these three ways into consideration, we find 24 possible sets of r_{0j}, depending on which of the eight ionizable groups in six-side chains (three per strand) is taken as the zeroth site.[38]. We approximated r_{0j} by the arithmetic mean[39] of the 24 sets of r_{0j} to calculate u_j. At $C_s = 0.01$ M, the sum over j in eq 6 converged at $j \sim 40$, which corresponds to as large a contour distance as 14 nm.

The calculated results are shown by thick solid lines in Figure 5 (pK_0 is again chosen properly for either sample at each C_s). These lines for the two higher C_s fit closely the xanthan data at the corresponding C_s, but those for the lower C_s deviate markedly upward. Thus, we find that although eq 6 with eq 8 describes the titration behavior of xanthan better than does eq 3 for the uniformly charged

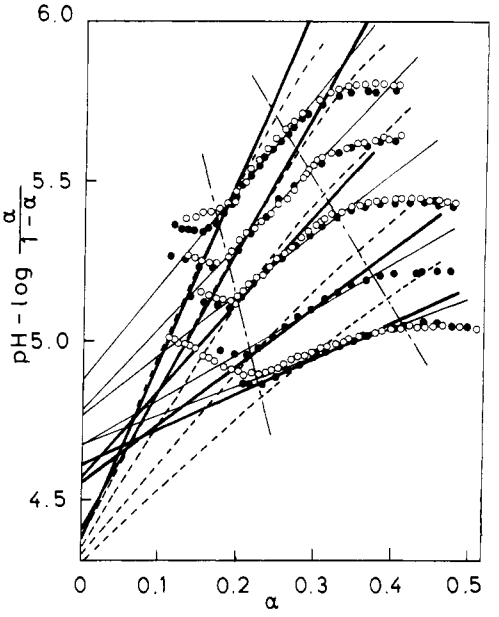

Figure 7. Comparison between theory and experiment: circles, data of Muroga et al.[24] for α-helical poly(glutamic acid) at C_s = 0.01, 0.02, 0.05, 0.1, and 0.2 M from top to bottom (different symbols signify different c_p); dashed lines, theoretical values[24] for a uniformly charged cylinder with $a = b = 0.9$ nm (equivalent to eq 3); thick solid lines, eq 6 (to $j = \infty$) with eq 8; thin solid lines, eq 6 (to $j = 7$) with eq 8. See the text as for the significance of the dot-dashed lines.

cylinder model, it is incomplete, overestimating considerably the electrostatic potential at the lower C_s of 0.01 and 0.02 M. This overestimate is most likely due to the DH approximation eq 8, since as mentioned above, eq 6 should be a very good approximation to the complete Ising result, at least for double-helical xanthan.

The thin solid lines in Figure 5 represent the theoretical values calculated from eq 6, with the sum taken only to $j = 4$. Their close fits to the data points imply that the above-mentioned overestimate of the total potential amounts to $-2\alpha\sum_{j=5}\log u_j$. The values of pK_0 chosen to force these lines to fit the xanthan data at given C_s differed slightly for the two samples probably owing to experimental error. The averages of pK_0 for the two samples were 2.81 (±0.03), 2.74 (±0.01), 2.61 (±0.01), and 2.53 (±0.01) at C_s = 0.01, 0.02, 0.05, and 0.1 M, respectively. These pK_0 values may be compared favorably with the experimental estimates (2.8 and 2.6 at 0.01 and 0.2 M, respectively) by Holzwarth,[40] who titrated xanthan in aqueous NaCl down to $\alpha = 0.2$ using HCl. This close agreement in pK_0 suggests that eq 6 (to $j = 4$) with eq 8 should describe well the titration behavior of the xanthan double helix down to very low α, though the truncation of the sum has no significance more than empirical data fitting.

C. Analysis of PGA Data. Nagasawa and co-workers[3,23,24] and Sugai and Nitta[6] found that titration data for α-helical poly(D- or L-glutamic acid) (PGA) in aqueous NaCl were fitted fairly closely by theoretical curves for the uniformly charged cylinder model when b (=a) was chosen to be 1.4 nm, a radius roughly twice that (0.65 nm)[24,35] expected for the α-helix. This descrepancy in helix radius is similar to what was found for xanthan (about a factor of 3) in this work when theoretical curves for the cylinder model were forced to fit the data. Thus, it is intriguing to analyze the PGA data in terms of eq 6, as has been done for xanthan.

In Figure 7, the thin and thick solid lines representing the theoretical values calculated to $j = 7$ and ∞, respec-

tively, are compared with the PGA data of Muroga et al.[24] in aqueous NaCl of different C_s's. In these calculations, we have used the relation[35] $r_{0j} = [0.845[1 - \cos(5j\pi/9)] + 0.0225j^2]^{1/2}$ nm for α-helical PGA; note that the smallest r_{0j} is 0.75 nm for $j = 4$. The two dot-dashed lines shown in the figure bound the range of α in which the α-helical conformation of PGA is maintained.[24] In this range, the fits of the thin lines are satisfactory at any C_s indicated, but those of the thick lines are limited to the two highest C_s's. Thus, we find also for α-helical PGA that eq 6 with the DH approximation overestimates the total potential at $C_s \lesssim 0.05$ M.

The dashed lines in Figure 7 represent the theoretical values computed by Muroga et al. for a uniformly charged cylinder with $a = b = 0.9$ nm (the radius of Na ions 0.25 nm + the helix radius 0.65 nm). Their poor agreement with the data indicates that at least in the range of C_s examined, the uniformly smeared charge distribution is a crude approximation for the PGA helix, as is the case for the xanthan helix.

Concluding Remarks

We have found that a titration equation, eq 6, for a discrete-charge model, combined with the DH approximation to pair interaction potentials, describes the data for double-helical xanthan and α-helical PGA at $C_s \gtrsim 0.05$ M but significantly overestimates the total interaction potential at lower C_s. To obtain agreement, the contributions from distant charges [$j \geq 5$ in eq 6 ($r_{0j} \gtrsim 2.5$ nm) for xanthan and $j \geq 8$ ($r_{0j} \gtrsim 1.45$ nm) for PGA] to the total potential had to be ignored completely. A literal explanation for this finding within the framework of the DH approximation is that at the lower C_s the electrostatic repulsion between ionized groups in either helix is screened considerably by "counterion condensation".

Manning and Holtzer[12] and also Manning,[14] applying Manning's ion condensation theory,[41] derived approximate titration equations and showed that their theoretical curves of ΔpK vs. α have an inflection or a discontinuity at α_1, a critical α value above which ion condensation is predicted to occur. However, neither such inflection nor discontinuity has ever been observed experimentally. For the helices of xanthan and PGA, even α_1 cannot unambiguously be determined from the Manning theory, which is based on the infinite line charge model. The reason is as follows.

Manning's criterion[41] for α_1 is written

$$\alpha_1 = DkTl/e^2 \tag{11a}$$

or

$$\alpha_1 = DkT/e^2\sigma \tag{11b}$$

where l is the length per unit charge or the average charge spacing at $\alpha = 1$. Equation 11a predicts that if $l > 0.72$ nm (in water at 25 °C), $\alpha_1 > 1$ and hence no ion condensation occurs even in the fully neutralized state; note that the closest charge distances for the xanthan double helix (0.78 nm) and the PGA helix (0.75 nm) are greater than this critical l value. On the other hand, if eq 11b is applied, α_1 is found to be 0.49 for the xanthan helix ($\sigma = 2.85$ nm^{-1}) and 0.21 for the PGA helix ($\sigma = 6.67$ nm^{-1}). These α_1 values do not seem to be compatible with what is predicted by eq 11a. This stems from the fact that the ionizable groups in either helix are present not on a line along the helix axis but on the surface of the helix with finite thickness. The point is that a line charge model chain equivalent to either helix must have too small an l ($=\sigma^{-1}$), i.e., 0.35 nm for xanthan and 0.15 nm for PGA. Hence, this model is inapplicable to helical xanthan and PGA, and α_1 estimated from eq 11b cannot be considered acceptable for the discrete charge model with which we are concerned here.

In conclusion, the theory of potentiometric titration for discretely charged rods is yet quite unsatisfactory and needs further elaboration toward the complete description of the titration behavior of intrinsically rigid polyelectrolytes.

Acknowledgment. We thank Emeritus Professor H. Fujita, Professor A. Teramoto, and Dr. H. Ohnuma for their advice and interest in this work. We learned much about potentiometric titration from Professor M. Nagasawa (now at Toyota Institute of Technology), Professor I. Noda, and Dr. Y. Muroga of Nagoya University, to whom many thanks are due. L. Zhang gratefully acknowledges the support of the Japan Society for the Promotion of Science. This work was supported by a Grant-in-Aid for Scientific Research from the Ministry of Education and by the Institute of Macromolecular Research, Osaka University.

Appendix

In this appendix, we derive eq 9 for a rigid polyacid with N (infinitely large) ionizable groups located at fixed points on the chain, first using a Bethe approximation and then successively raising the approximation at a particular α of $^1/_2$. We specify the charge state of group or site i ($i = 1, 2, ..., N$) by a variable ζ_i, which can be either 1 (ionized) or 0 (unionized). Assuming that the total interaction energy is the sum of pair electrostatic interaction potentials $w_{i,j}$, we may write the grand partition function Ξ for the polyacid as

$$\Xi = \sum_{\zeta_1=0,1}\sum_{\zeta_2=0,1}\cdots\sum_{\zeta_N=0,1}\lambda^{\sum_{i=1}^{N}\zeta_i}\exp\left[-\frac{1}{kT}\left[\sum_{i=1}^{N-1}w_{i,i+1}\zeta_i\zeta_{i+1} + \sum_{i=1}^{N-2}\sum_{j=i+2}^{N}w_{i,j}\zeta_i\zeta_j\right]\right] \tag{A-1}$$

where λ is the absolute activity related to ΔpK by[8,9,15,35]

$$\log\lambda = \Delta pK + \log(\alpha/1-\alpha) \tag{A-2}$$

As a first approximation (Bethe approximation), we replace $\sum_j w_{i,j}\zeta_i\zeta_j$ by a mean-field approximation value, i.e.,

$$\sum_{j=i+2}^{N} w_{i,j}\zeta_i\zeta_j = w_i'\zeta_i \tag{A-3}$$

where

$$w_i' = \sum_{j=i+2}^{N} w_{i,j}\bar{P}_j \tag{A-4}$$

with $\bar{P}_j$ being the "a priori average probability" that group j is ionized. For infinitely large N, w_i' may be considered independent of i, so that eq A-1 is simplified to give

$$\Xi = \sum_{\zeta 1}\sum_{\zeta 2}\cdots(\upsilon\lambda)^{\sum_i\zeta_i}u_1^{\sum_i\zeta_i\zeta_{i+1}} \tag{A-5}$$

where

$$u_1 = \exp(-w_{i,i+1}/kT) \tag{A-6}$$

$$\upsilon = \exp(-w_i'/kT) = \exp\left(-\sum_{j=i+2}^{\infty} w_{i,j}\bar{P}_j/kT\right) \tag{A-7}$$

In eq A-5, we have assumed that u_1 is the same for any i; this ensures that identical υ can be assigned to any i.

The partition function given by eq A-5 has the same form as that in the first nearest-neighbor Ising model, and α ($=\partial \ln \Xi/N\,\partial \ln\lambda$) or $\langle P_i\rangle$ (the average probability that group i is ionized) is calculated by the established method to be[42]

$$\alpha = \langle P_i \rangle = \frac{v\lambda[u_1^2 v\lambda - u_1 + 2 + u_1[(u_1 v\lambda - 1)^2 + 4v\lambda]^{1/2}]}{(u_1 v\lambda - 1)^2 + 4v\lambda + (u_1 v\lambda + 1)[(u_1 v\lambda - 1)^2 + 4v\lambda]^{1/2}} \quad \text{(A-8)}$$

The mean-field approximation made above requires the self-consistency that $\bar{P}_j$ in the defining equation of v (A-7) is equal to $\langle P_i \rangle$ ($=\alpha$). Thus, eq A-8 with $v = \exp(\alpha \sum_j w_{ij}/kT)$ determines α, but what we need here is the solution for λ as a function of α (see eq A-2). This reads

$$\lambda = [1 + x u_1^{-1} \pm [(1 + x u_1^{-1})^2 - 1]^{1/2}]/u_1 v \quad \text{(A-9)}$$

where x is defined by eq 10 and the sign $\pm$ is determined to be + for $\alpha > 0.5$ and − for $\alpha < 0.5$ by the condition that, for any polyacid, $\partial \mathrm{pH}/\partial\alpha > 0$ and hence $\partial\lambda/\partial\alpha > 0$ regardless of positive u_1 and v (see also ref 10).

Substituting eq A-9 into eq A-2 and noting that $v = (u_2 u_3 \ldots)^{\alpha}$, we get

$$\Delta \mathrm{p}K_1 = \log [[(1-\alpha)/\alpha] \times [1 + x u_1^{-1} \pm [(1 + x u_1^{-1})^2 - 1]^{1/2}] u_1^{-1}] - \alpha \sum_{j=2} \log u_j \quad \text{(A-10)}$$

where the subscript 1 attached to $\Delta \mathrm{p}K$ signifies the first approximation. At the midpoint of titration, i.e., $\alpha = {}^1/_2$ at which x vanishes, eq A-10 reduces to

$$\Delta \mathrm{p}K_1{}^* \equiv \Delta \mathrm{p}K_1(\alpha = {}^1/_2) = -\log u_1 - (1/2) \sum_{j=2} \log u_j \quad \text{(A-11)}$$

In our second approximation, $w_{i,i+1}$ and $w_{i,i+2}$ are retained, with all other higher order interactions incorporated into the mean-field potential. If the characteristic equation derived by Lifson et al.[11] for the second nearest-neighbor case is used, $\Delta \mathrm{p}K_2{}^*$, i.e., $\Delta \mathrm{p}K$ at $\alpha = {}^1/_2$ in the second approximation, is evaluated to be

$$\Delta \mathrm{p}K_2{}^* = -\log u_1 - \log u_2 - (1/2) \sum_{j=3} \log u_j \quad \text{(A-12)}$$

Evidently, our Nth approximation is to treat all pairs of potentials without mean-field approximation. At $\alpha = {}^1/_2$ the chemical potential ($=kT \ln \lambda$) of a given ionized group 0 (relative to that in the nonionized state) equals the total interaction energy $\sum_{j=1} w_{0j}$ for the group,[43] so that we have

$$\lambda^{-1} = \prod_{j=1} u_j \qquad (\text{at } \alpha = {}^1/_2) \quad \text{(A-13)}$$

which, on substitution into eq A-2 with $\alpha = {}^1/_2$, yields

$$\Delta \mathrm{p}K_N{}^* = -\sum_{j=1} \log u_j \quad \text{(A-14)}$$

Comparison of this with eq A-11 shows that the first approximation underestimates $\Delta \mathrm{p}K$ by $-\alpha \sum_{j=2} \log u_j$ at $\alpha = {}^1/_2$. If Lifson et al.'s theorem[11] that the curve of $\Delta \mathrm{p}K$ vs. α derived from Ξ is symmetrical about the midpoint of titration is used along with the fact that $\Delta \mathrm{p}K$ vanishes at $\alpha = 0$, $\Delta \mathrm{p}K_1$ is found to be smaller by $-\alpha \sum_{j=2} \log u_j$ than the "exact" $\Delta \mathrm{p}K$ ($=\Delta \mathrm{p}K_N$) in the fully ionized state too. Thus, addition of $-\alpha \sum_{j=2} \log u_j$ to the right-hand side of eq A-10 yields an expression (eq 9) that gives exactly the same $\Delta \mathrm{p}K$ values as those from the complete Ising method at $\alpha = {}^1/_2$ and 1.

Registry No. Xanthan gum, 11138-66-2.

References and Notes

(1) Overbeek, J. T. G. *Bull. Soc. Chim. Belg.* **1948**, *57*, 252.
(2) Katchalsky, A.; Shavit, N.; Eisenberg, H. *J. Polym. Sci.* **1954**, *13*, 69.
(3) Nagasawa, M. *Pure Appl. Chem.* **1971**, *26*, 519.
(4) Kotin, L.; Nagasawa, M. *J. Chem. Phys.* **1962**, *36*, 873.
(5) Kawaguchi, Y.; Nagasawa, M. *J. Phys. Chem.* **1969**, *73*, 4382.
(6) Sugai, S.; Nitta, K. *Biopolymers* **1973**, *12*, 1363.
(7) Stigter, D. *J. Colloid Interface Sci.* **1975**, *53*, 296.
(8) Rice, S. A.; Nagasawa, M. In *Polyelectrolyte Solutions*; Academic: New York and London, 1961.
(9) Harris, F. E.; Rice, S. A. *J. Phys. Chem.* **1954**, *58*, 725.
(10) Lifson, S. *J. Chem. Phys.* **1957**, *26*, 727.
(11) Lifson, S.; Kaufman, B.; Lifson, H. *J. Chem. Phys.* **1957**, *27*, 1356.
(12) Manning, G. S.; Holtzer, A. *J. Phys. Chem.* **1973**, *77*, 2206.
(13) Sasaki, S.; Minakata, A. *Biophys. Chem.* **1980**, *11*, 199.
(14) Manning, G. S. *J. Phys. Chem.* **1981**, *85*, 870.
(15) Cleland, R. L. *Macromolecules* **1984**, *17*, 634.
(16) Paradossi, G.; Brant, D. A. *Macromolecules* **1982**, *15*, 874.
(17) Sato, T.; Norisuye, T.; Fujita, H. *Polym. J.* **1984**, *16*, 341.
(18) Sato, T.; Kojima, S.; Norisuye, T.; Fujita, H. *Polym. J.* **1984**, *16*, 423.
(19) Sato, T.; Norisuye, T.; Fujita, H. *Macromolecules* **1984**, *17*, 2696.
(20) Liu, W.; Sato, T.; Norisuye, T.; Fujita, H. *Carbohydr. Res.* **1987**, *160*, 267.
(21) Coviello, T.; Kajiwara, K.; Burchard, W.; Dentini, M.; Crescenzi, V. *Macromolecules* **1986**, *19*, 2826.
(22) Sho, T.; Sato, T.; Norisuye, T. *Biophys. Chem.* **1986**, *25*, 307.
(23) Nagasawa, M.; Holtzer, A. *J. Am. Chem. Soc.* **1964**, *86*, 531.
(24) Muroga, Y.; Suzuki, K.; Kawaguch, Y.; Nagasawa, M. *Biopolymers* **1972**, *11*, 137.
(25) Cleland, R. L.; Wang, J. L.; Detweiler, D. M. *Macromolecules* **1982**, *15*, 386.
(26) Zhang, L.; Liu, W.; Norisuye, T.; Fujita, H. *Biopolymers* **1987**, *26*, 333.
(27) Though widely accepted, this method assumes that at a given pH and C_s, the activity coefficient of free hydrogen ions in the xanthan solution is equal to that in aqueous HCl.
(28) See ref 17 for the experimental procedure of determining $\mathrm{DS}_{\mathrm{pyr}}$.
(29) Olander, D. S.; Holtzer, A. *J. Am. Chem. Soc.* **1968**, *90*, 4549.
(30) Mandel, M. *Eur. Polym. J.* **1970**, *6*, 807.
(31) Hill, T. L. *Arch. Biochem. Biophys.* **1955**, *57*, 229.
(32) Okuyama, K.; Arnott, S.; Moorhouse, R.; Walkinshow, M. D.; Atkins, E. D. T.; Wolf-Ullish, Ch. In *Fiber Diffraction Methods*; French, A. D., Gardner, K. H., Eds.; ACS Symposium Series 141; American Chemical Society: Washington, DC, 1980; p 411.
(33) Ikegami, A. *J. Polym. Sci., Part A* **1964**, *2*, 907.
(34) Fixman, M. *J. Chem. Phys.* **1979**, *70*, 4995.
(35) Zimm, B. H.; Rice, S. A. *Mol. Phys.* **1960**, *3*, 391.
(36) Minakata, A.; Matsumura, K.; Sasaki, S.; Ohnuma, H. *Macromolecules* **1980**, *13*, 1549.
(37) The pyruvic acid groups, attached to the terminal mannose residues of the trisaccharide chains (see Figure 1), should have some freedom in solution, but for simplicity, their locations are assumed to be fixed, as indicated in Figure 6.
(38) It is assumed that the probability of ionization of any acid group in the xanthan double helix is determined only by electrostatic interactions with other groups. With this assumption, all the acid groups are treated without distinction.
(39) The mean r_{0j} values obtained are 1.88, 1.49, 1.86, 2.16, ... nm for $j = 1, 2, 3, 4, \ldots$; the ionizable groups are numbered along the helix axis, and the smallest r_{0j} appears at $j = 2$.
(40) Holzwarth, G. *Biochemistry* **1976**, *15*, 4333.
(41) Manning, G. S. *J. Chem. Phys.* **1969**, *51*, 924.
(42) See ref 9 or 10.
(43) This follows from Lifson et al.'s theory[11] which shows that μ ($\equiv kT \ln \lambda - \sum_{j=1} w_{0,j}$) at $1 - \alpha$ is equal to $-\mu$ at α. The cyclic condition used by these authors is equivalent to the condition that $N = \infty$.